

# Coordinated Control of Tractive and Braking Forces using High Slip for Improved Turning Performance of an Electric Vehicle equipped with In-wheel Motors

Wongun Kim

Program in Automotive Engineering  
Seoul National University  
Seoul, Korea  
virus3764@snu.ac.kr

Kyongsu Yi

Mechanical and Aerospace Engineering  
Seoul National University  
Seoul, Korea  
kyi@snu.ac.kr

**Abstract**—This paper describes development of coordinated control of tractive and braking forces using high wheel slip in order to enhance turning performance of electric vehicle equipped with in-wheel motors. In the case of conventional vehicle, turning radius is definitely limited by kinematic features with respect to wheel base, maximum steering angle and track width of the vehicle. Military and special purpose vehicles are required to overcome turning radius limitation in order to conduct urgent and emergency tasks and avoid enemies rapidly. The control purpose is achieved by minimizing lateral tire force of rear wheels using excessive wheel slip condition. It is possible for the vehicle to turn around central turning point using the proposed algorithm. The center turning point is defined based on the driver's intention. The coordinated control algorithm consists of three parts: an upper level controller that computes the desired net force and moment in order to make one point turning motion, a lower level controller distributes tractive and brake input torques of each wheel for excessive slip control and sensor/estimator provides vehicle information to controllers. Computer simulations have been conducted to evaluate performance of the proposed control algorithm. It has been shown from simulation results that turning performance can be significantly improved.

**Keywords** - electric vehicle; high wheel slip control; turning performance; in-wheel motor; torque distribution

## I. INTRODUCTION

By combining conventional power system with an electric drive, advanced hybrid electric systems and rechargeable energy storage, hybrid electric vehicles (HEVs) add a flexible new dimension to various functions for improvement of driving performance. The electric system gives a number of advantages, including volume efficiency, fuel efficiency, reduced life cycle costs, reduced environmental impact and increased silent driving characteristics. By virtue of the recent development of the hybrid systems and in-wheel-motors, drive and brake torque can be independently determined.

In the case of conventional vehicle, turning radius is definitely limited by kinematic features with respect to wheel base, maximum steering angle and track width. In the case of military and special purpose vehicle, it is necessary to overcome turning radius limitation in order to conduct urgent and emergency tasks and avoid enemies rapidly. In previous

studies, four wheel steering control system was investigated to decrease turning radius and not developed for conventional vehicles because of space and cost problems. In recently electric vehicle industry, series hybrid systems and in-wheel motors have been developed to improve driving performance and energy efficiency<sup>[1],[2]</sup>.

In this paper, the proposed electric vehicle is equipped with in-wheel motors, independent hydraulic brake and series hybrid power system. Drive and brake torques can be independently generated. Strategy of a coordinated control algorithm is lateral tire force minimization using excessive wheel slip condition, which is similar to skills of an expert race driver. If wheel slip ratio increases significantly, lateral tire force of rear axle converges to small value and status of vehicle becomes artificial over-steer. Therefore, vehicle is possible to turn around central point which is defined by driver's intention. The coordinated control algorithm consists of three parts: an upper level controller that computes the desired net force and moment in order to make one point turning motion, a lower level controller distributes drive and brake input torques of each wheel for excessive slip control and sensor/estimator provides vehicle information to controllers.

## II. CONTROL SYSTEM DEFINITION

### A. System Overview

The proposed vehicle is equipped with in-wheel motors and hydraulic brake system which can generate drive and brake torque independently. Electric power system consists of battery, engine-generator and inverter. This power system transfers electric power to in-wheel motors as shown in figure 1.

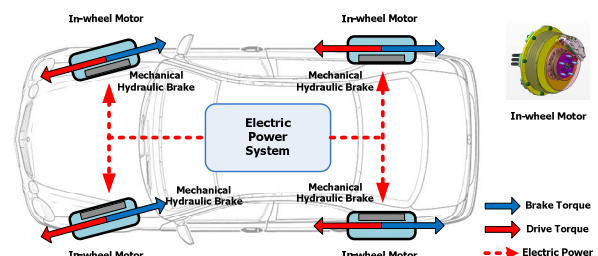


Figure 1. Configuration and power flow of electric vehicles

### B. Control Objectives and Strategy

In case the case of conventional vehicle, turning radius is definitely limited by kinematic features with respect to wheel base, maximum steering angle and track width.

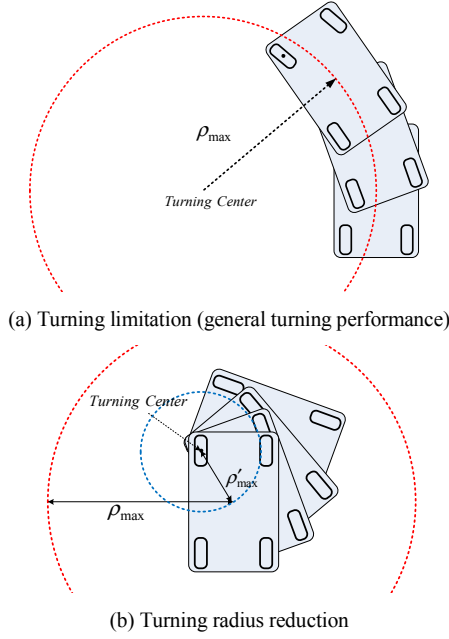


Figure 2. Control Scheme

It is necessary to overcome turning radius limitation related to mechanical structure in order to conduct urgent, emergency tasks and avoid enemies rapidly in military and special purpose vehicles as shown in figure 2.

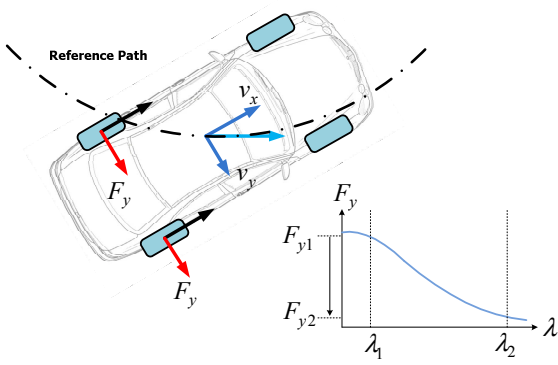


Figure 3. Control Strategy with high wheel slip on rear wheels

Strategy of a coordinated control algorithm is lateral tire force minimization using excessive wheel slip condition. If wheel slip ratio increases significantly ( $\lambda_1 \rightarrow \lambda_2$ ), lateral tire force of rear axle converges to small values and status of vehicle becomes artificial over-steer maneuver as shown in figure 3.

### C. Control Architecture

A coordinated control algorithm is designed to improve turning performance of electric vehicle using independent wheel torque with high wheel slip conditions. An upper level, lower level controller and sensor/estimator are included in control system as shown in figure 4. A desired dynamics determination and sliding control algorithm are included in an upper level control. A lower level control consists of a high slip control and torque distribution algorithm. The desired dynamics determination algorithm computes desired velocity from driver's turning center and desired yaw rate commands. The required net force and yaw moment are defined to follow the desired velocity and based on sliding control method. In order to minimize resistance lateral tire force and satisfy the desired lateral tire force, the high slip control algorithm generates high wheel slip condition on rear axle and determines the required rear wheel torque inputs. The torque distribution algorithm coordinates drive and brake torques using the fixed-point control allocation method. Functions of block diagram and control input and outputs are described in table 1. In this paper, sensor and estimator is not included. Vehicle velocity, wheel angular velocity and tire force information can be directly obtained in vehicle dynamic model. Tire force estimation will be conducted in next research.

TABLE I. COORDINATED CONTROL ALGORITHM FUNCTION TABLE

Classification	Function	Input	Output
Desired dynamics	Desired velocity determination	- Turning center - desired yaw rate	- Desired velocity
Sliding control	Determination of reference desired net force & yaw moment	- desired velocity - measured velocity and yaw rate	- required net forces (lateral, longitudinal and yaw moment)
High slip control	Calculation of wheel torque for high slip	- required lateral, longitudinal force and yaw moment - velocity - wheel velocity	- Rear wheel input torque
Torque distribution	Distribution wheel torque inputs	- rear wheel input torque - tire force information	- front wheel input torque

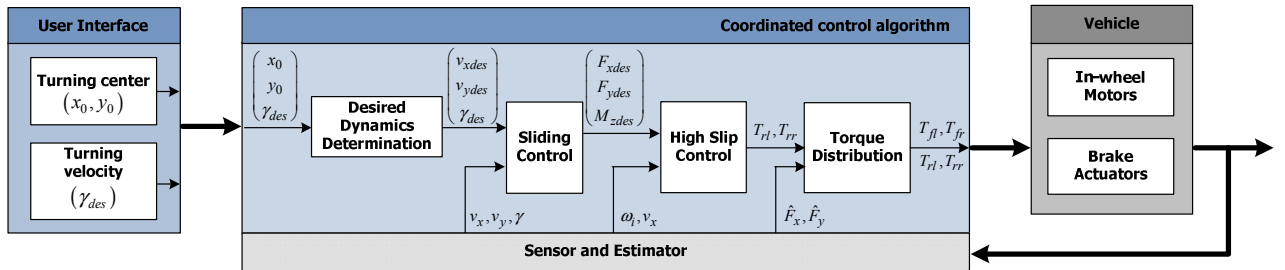


Figure 4. Block diagram of the coordinated control algorithm

### III. VEHICLE DYNAMIC AND ACTUATOR MODEL

#### A. Vehicle Dynamic Model

The TruckSim is used for simulation of dynamic modeling in this research. The full vehicle dynamic model of the TruckSim makes it possible to analyze a vehicle's various maneuvers and to study the coordinated control algorithm. A vehicle model consists of 18 DOF such as translational and rotational dynamic models of the sprung mass, 4 suspension models, 4 wheel dynamics models and 4 steering dynamic models. Wheel dynamics contains in-wheel motor, brake system and tire model. Table 2 shows chassis specifications of an electric vehicle such as mass, track width, front/rear wheelbase, wheel radius, z-axis moment of inertia and etc.

TABLE II. SPECIFICATION OF A ELECTRIC VEHICLE

Vehicle Parameters	Specification	Vehicle Parameters	Specification
Sprung mass	2210 [kg]	Wheel base	3.32 [m]
Moment of inertia	4331.6 [kgm <sup>2</sup> ]	Wheel moment of inertia	13 [kgm <sup>2</sup> ]
Wheel radius	0.56 [m]	Track width	1.9 [m]

#### B. Motor Dynamic Model

The target vehicle equipped with in-wheel-motors is able to operate differential driving and braking modes. Capacity of in-wheel motor is 30kW. Figure 5 (a) shows a performance curve and efficiency of wheel-in-motors and (b) illustrates wheel-in-motor structure.

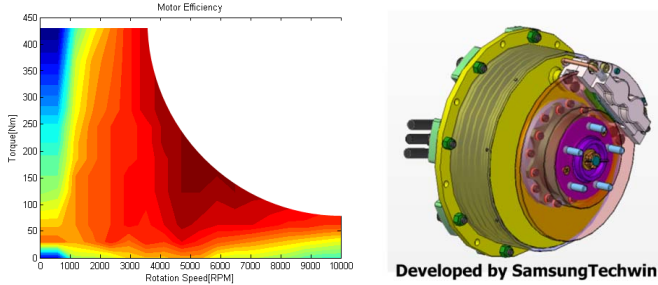


Figure 5. Example of a figure caption. (figure caption)

In-wheel motor model operates in the following manner; control input is the desired output torque which is distributed from the lower level controller and output of the motor model is the generating torque. The relation between output and input torques of in-wheel-motor is modeled using first order transfer function and time constant of in-wheel motor is set to 0.05 as follows:

$$G(s) = \frac{\text{output torque}}{\text{input torque}} = \frac{1}{s \cdot \tau_{\text{motor}} + 1} \quad (1)$$

### IV. DESIGN OF THE COORDINATED CONTROL ALGORITHM

Coordinated control algorithm consists of the desired dynamics, sliding, high slip control and torque distribution.

#### A. Determination of the Desired Dynamics

Turning center point and desired yaw rate are determined as driver's control inputs. The desired longitudinal and lateral velocity need to be calculated to turn around center point. The process of the desired velocity determination is illustrated as shown in figure 6.

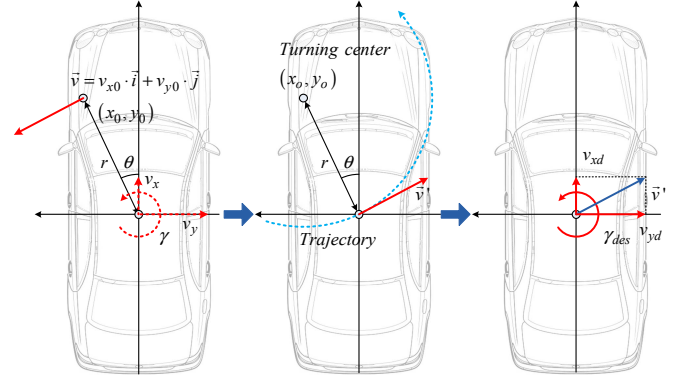


Figure 6. Determination of longitudinal and lateral velocity

Velocity ( $\vec{v}$ ) at point  $(x_0, y_0)$  is defined as longitudinal and lateral velocity and yaw rate of the vehicle mass center. Also, it is related to distance and angle between mass center and turning center as follows:

$$\begin{aligned} \vec{v} &= v_x \cdot \vec{i} + v_y \cdot \vec{j} - r \cdot \gamma \sin \theta \cdot \vec{i} + r \cdot \gamma \cos \theta \cdot \vec{j} \\ &= v_{x0} \cdot \vec{i} + v_{y0} \cdot \vec{j} \end{aligned} \quad (2)$$

$$v_{x0} = v_x - r \cdot \gamma \sin \theta$$

$$v_{y0} = v_y + r \cdot \gamma \cos \theta.$$

If point  $(x_0, y_0)$  is turning center, longitudinal and lateral velocity at turning center point can be set to zero as follows:

$$\begin{aligned} \vec{v} &= v_{x0} \cdot \vec{i} + v_{y0} \cdot \vec{j} = \vec{0}, \text{ where center point is } (x_0, y_0) \\ v_{x0} &= v_x - r \cdot \gamma \cos \theta = 0 \\ v_{y0} &= v_y + r \cdot \gamma \sin \theta = 0 \end{aligned} \quad (3)$$

The desired velocity ( $\vec{v}'$ ) of the vehicle can be obtained and defined as the desired longitudinal velocity ( $v_{xd}$ ) and lateral velocity ( $v_{yd}$ ) as follows:

$$\begin{aligned} \vec{v}' &= v_{xd} \cdot \vec{i} + v_{yd} \cdot \vec{j} \\ \text{where, } v_{xd} &= -r \cdot \gamma_{des} \sin \theta, v_{yd} = r \cdot \gamma_{des} \cos \theta. \end{aligned} \quad (4)$$

#### B. Sliding Control Algorithm

To track the desired velocity and yaw rate, the sliding control is designed based on vehicle dynamics as follows:

$$\dot{x} = \begin{bmatrix} x_2 x_3 \\ -x_1 x_3 \\ 0 \end{bmatrix} + \text{diag} \left[ \frac{1}{m} \quad \frac{1}{m} \quad \frac{1}{I_z} \right] \cdot \begin{bmatrix} F_{xd} \\ F_{yd} \\ M_{zd} \end{bmatrix}. \quad (5)$$

$$\text{where, } x = \begin{bmatrix} v_x & v_y & \gamma \end{bmatrix}^T = \begin{bmatrix} x_1 & x_2 & x_3 \end{bmatrix}^T$$

States of dynamics are longitudinal velocity ( $v_x$ ), lateral velocity ( $v_y$ ) and yaw rate ( $\gamma$ ) of the vehicle. Sliding surfaces are defined and  $W$  are weighting factors as follows:

$$\begin{aligned} s_1 &= W_1 (x_1 - x_{1d}) \\ s_2 &= W_2 (x_2 - x_{2d}) \\ s_3 &= W_3 (x_3 - x_{3d}). \end{aligned} \quad (6)$$

The control objective is to keep the surface  $s$  at zero and it can be achieved by choosing the control law satisfying sliding condition.

$$\frac{1}{2} \frac{d}{dt} s^2 \leq -\eta |s| \quad \text{where, } \eta \text{ is positive value} \quad (7)$$

Derivatives of sliding surface can be written by the desired dynamics and vehicle dynamic equation (5) as follows:

$$\begin{aligned} \dot{s}_1 &= W_1 \cdot \dot{x}_1 - W_1 \cdot \dot{x}_{1d} = W_1 \left( x_2 x_3 + \frac{1}{m} F_{xd} \right) - W_1 \cdot \dot{x}_{1d} \\ &\leq -\eta_1 \operatorname{sgn}(s_1) \end{aligned} \quad (8)$$

$$\begin{aligned} \dot{s}_2 &= W_2 \cdot \dot{x}_2 - W_2 \cdot \dot{x}_{2d} = W_2 \left( -x_1 x_3 + \frac{1}{m} F_{yd} \right) - W_2 \cdot \dot{x}_{2d} \\ &\leq -\eta_2 \operatorname{sgn}(s_2) \end{aligned} \quad (9)$$

$$\begin{aligned} \dot{s}_3 &= W_3 \cdot \dot{x}_3 - W_3 \cdot \dot{x}_{3d} = W_3 \left( \frac{M_{zd}}{I_z} \right) - W_3 \cdot \dot{x}_{3d} \\ &\leq -\eta_3 \operatorname{sgn}(s_3). \end{aligned} \quad (10)$$

The sliding control law is obtained as the desired longitudinal and lateral net force and yaw moment.

$$F_{xd} = m \left[ \dot{x}_{1d} - \frac{\eta_1}{W_1} \operatorname{sat} \left( \frac{s_1}{\phi_1} \right) - x_2 x_3 \right] \quad (11)$$

$$F_{yd} = m \left[ \dot{x}_{2d} - \frac{\eta_2}{W_2} \operatorname{sat} \left( \frac{s_2}{\phi_2} \right) + x_1 x_3 \right] \quad (12)$$

$$M_{zd} = I_z \left[ \dot{x}_{3d} - \frac{\eta_3}{W_3} \operatorname{sat} \left( \frac{s_3}{\phi_3} \right) \right] \quad (13)$$

### C. High Slip Control Algorithm

Control objective is minimization of lateral resistance tire force using excessive wheel slip condition. The desired wheel slip ratio can be determined to keep lateral tire force error to zero as follows:

$$\lambda_d(k+1) = \lambda_d(k) + k_1 \left| \hat{F}_y - F_{yd} \right|. \quad (14)$$

The desired rear wheel input torques are calculated based on PID control algorithm as follows:

$$\begin{aligned} T_{RL,RR} &= K_{Pslip} (\lambda_d - \lambda) + K_{Dslip} \frac{d}{dt} (\lambda_d - \lambda) \\ &\quad + K_{Islip} \int (\lambda_d - \lambda) dt. \end{aligned} \quad (15)$$

### D. Torque Distribution Algorithm

A fixed-point control allocation (CA) method originally proposed by Lu<sup>[3]</sup> and Burken<sup>[4]</sup> was used to solve the control allocation problem with respect to nonlinear system control for aircraft. And then, Wang<sup>[5]</sup> applied this method to optimal distribution for ground vehicles. In this paper, this method is useful for independent driving system equipped with in-wheel motors and hydraulic brake system. Control inputs are drive and brake wheel torque ( $T_b, P_{bi}, i=1,2$ ) of the proposed vehicle. Those can be generated to track the desired net longitudinal force and yaw moment which is determined sliding control algorithm. The desired dynamics and control inputs are related as follows:

$$\begin{aligned} \begin{bmatrix} F_x \\ M_z \end{bmatrix} &= \frac{1}{r_w} \begin{bmatrix} \cos \delta_f \\ (L_f \sin \delta_f - t_w \cos \delta_f) \end{bmatrix} \begin{bmatrix} 1 & 1 & 1 & 1 \end{bmatrix} \\ \cdot \begin{bmatrix} T_1 & T_2 & P_{b1} & P_{b2} \end{bmatrix}^T &= B \cdot u. \end{aligned} \quad (16)$$

The control input of the fixed-point control allocation is determined to minimize the performance index as follows:

$$\min J = \frac{1}{2} (Bu - v_d)^T W_v (Bu - v_d) + \frac{1}{2} \epsilon u^T W_u u. \quad (17)$$

subject to  $u_{\min} < u < u_{\max}$

$$\begin{aligned} \text{where, } u &= \begin{bmatrix} T_1 & T_2 & P_{b1} & P_{b2} \end{bmatrix}^T, v_d = \begin{bmatrix} F_{xd} & M_{zd} \end{bmatrix}^T \\ u_{\min} &= \max \left[ u_{\min}, u(t - T_{\text{sampling}}) + T_{\text{sampling}} \cdot r_{\min} \right] \\ u_{\max} &= \min \left[ u_{\max}, u(t - T_{\text{sampling}}) + T_{\text{sampling}} \cdot r_{\max} \right] \end{aligned}$$

$T_{\text{sampling}}$  is sampling time,  $r_{\min}$  and  $r_{\max}$  are the lower and upper bounds of actuation rate limits, respectively.  $\epsilon$  is small value used to balance between allocation error and actuation cost.  $u_{\min}, u_{\max}$  denotes the lower and upper bounds of actuation magnitude limits, respectively. These limits depend not only on wheel conditions but also on fault status of in-wheel motors. Detail contents of wheel conditions contain angular velocity, tire normal force and friction coefficient between tire and road.  $v_d$  denotes the desired dynamic matrix and  $B$  matrix represents relation between the desired dynamics and control inputs. Weighting factors need to be defined to balance between virtual control input and distributed control inputs as follows:

$$W_u = \operatorname{diag}[\sigma_1 \quad \sigma_2 \quad \sigma_3 \quad \sigma_4], W_v = \operatorname{diag}[\kappa_1 \quad \kappa_2] \quad (18)$$

The fixed-point control allocation algorithm iterates according to the equation as follows:

$$u_{k+1} = \operatorname{sat} \left[ (1 - \epsilon) \eta B_{k-1}^T W_v v_d - (\eta T - I) u_k \right] \quad (19)$$

where,  $T = (1 - \varepsilon)\eta B_{k-1}^T W_v B_{k-1} + \varepsilon W_u$ ,  $\eta = 1/\|T\|_F$ ,

$$\|T\|_F = \left( \sum_{i=1}^p \sum_{j=1}^p t_{ij}^2 \right)^{\frac{1}{2}}$$

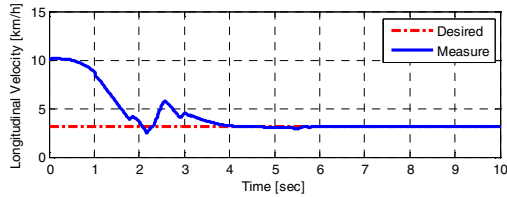
Text heads organize the topics on a relational, hierarchical basis.  $T$  is a symmetric matrix,  $\eta = 1/\|T\|_F$ ,  $t_{ij}$  are the elements of matrix  $T$ , with  $\|T\|_F$  being the Frobenius norm of matrix  $T$ . Saturation function,  $sat$ , clips the elements of the control vector according to

$$sat(u) = \begin{cases} \bar{u}_i, & u_i \geq \bar{u}_i \\ u_i, & \underline{u}_i \leq u_i \leq \bar{u}_i, \quad i = 1, 2, 3, 4 \\ \underline{u}_i, & u_i \leq \underline{u}_i \end{cases} \quad (20)$$

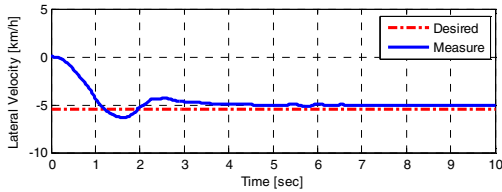
Compared with the other QP-based control allocation methods such as active-set and primal-dual interior-point, one of the advantages of the fixed-point is its extremely low computational effort. It is clear that the fixed-point control allocation method has much lower computational burden, which is very attractive for real-time control systems.

## V. SIMULATION RESULTS

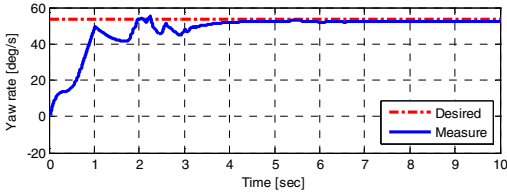
Numerical simulations have been conducted using Trucksim dynamic model. Turning center point is set to front wheel ( $x_0 = 1.65$ ,  $y_0 = 0.95$ ). Friction coefficient between tire and road is 0.6 and initial velocity is 10 km/h. Figure 7 (a), (b), (c) shows that sliding surfaces converge to zero. Input torques (drive/brake) and trajectories are shown as figure 7 (d) and (e).



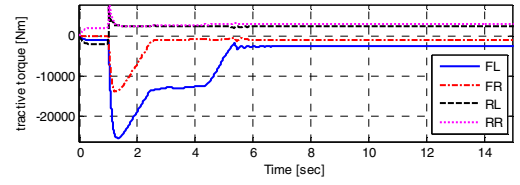
(a) Longitudinal velocity [km/h]



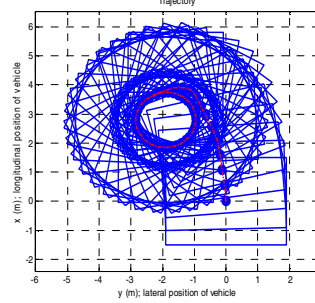
(b) Lateral velocity [km/h]



(c) Yaw rate [deg/s]



(d) Input torque [Nm]



(e) Trajectory

Figure 7. Simulation results

## VI. CONCLUSION

Coordinated control algorithm of tractive and braking forces using high slip has been designed to improve turning performance of electric vehicle equipped with in-wheel motors. Numerical simulations have been conducted to evaluate performance of the proposed control algorithm. It has been shown from simulation results that turning performance can be significantly improved.

## ACKNOWLEDGMENT

This work was supported by the Samsung Techwin, SNU-IAMD, the Korea Research Foundation Grant funded by the Korean Government (MEST)(KRF-2009-200-D00003), and National Research Foundation of Korea Grant funded by the Korean Government (2011-0001277).

## REFERENCES

- [1] Shino-ichiro Sakai, Hideo sado and Yoichi Hori, "Motion control in an electric vehicle with four independently driven in-wheel motors", IEEE/ASME transaction on mechatronics, Vol.4, No.1, pp. 9-16, 1999
- [2] Cong Geng, Lotfi Mostefai, Mouloud Denai and Yoichi Hori, "Direct Yaw-moment control of an in-wheel motored electric vehicle based on body slip angle fuzzy observer", IEEE/ASME transaction on mechatronics, Vol.56, No.5, pp.1141-1419, 2009
- [3] P. Lu, "Constrained tracking control of nonlinear systems," Syst. Control Lett., vol. 27, pp. 305-314, 1996.
- [4] Burken, Ping Lu, Zhenglu Wu, and Cathy Bahm, "Two reconfigurable flight-control design methods: Robust servomechanism and control allocation," , Journal of Guidance, Control and Dynamics, Vol.24, No.3, pp. 482-493, May-June 2001
- [5] Junmin Wang and Raul G. Longoria, "Coordinated vehicle dynamics control with control distribution", Preceeding of the 2006 American Control Conference, pp.5348-5353